Lab on a Chip

Accepted Manuscript

ROYAL SOCIETY OF CHEMISTRY

www.rsc.org/loc

Journal Name

COMMUNICATION

Mass Spectrometry-Based Monitoring of Millisecond Protein-Ligand Binding Dynamics Using an Automated Microfluidic Platform

Received 00th January 20xx,
Accepted 00th January 20xx

DOI: 10.1039/x0xx00000x

www.rsc.org/

Yongzheng Cong,[a] Shanta Katipamula,[a] Cameron D. Trader,[a] Daniel J. Orton,[b] Tao Geng,[a] Erin S. Baker,[b] and Ryan T. Kelly*[a]

Characterizing protein-ligand binding dynamics is crucial for understanding protein function and for developing new therapeutic agents. We present a novel microfluidic platform that features rapid mixing of protein and ligand solutions, variable incubation times, and an integrated electrospray ionization source for mass spectrometry-based monitoring of protein-ligand binding dynamics. This platform offers many advantages, including solution-based binding, label-free detection, automated operation, rapid mixing, and low sample consumption.

Noncovalent protein-ligand interactions are fundamental to many biological processes including signal transduction, enzymatic catalysis, and immune response. Determination of protein-ligand binding affinities and kinetics is critically important for drug discovery[1] and understanding protein function.[2] A number of analytical methods have been developed for protein-ligand studies including equilibrium dialysis, liquid chromatography, capillary electrophoresis (CE), surface plasmon resonance (SPR), spectroscopy, and calorimetry.[3] Many of these methods, however, require labelling or immobilization of one of the binding partners to a solid substrate, which can substantially interfere with the binding and can introduce additional complications such as costly assay development.

Mass spectrometry (MS) is increasingly being used for protein-ligand studies as it provides precise mass information and detailed quantitative information of unbound proteins and protein-ligand complexes without the need to incorporate a label or immobilize one of the binding partners.[4-6] While the use of MS for measuring equilibrium binding affinities continues to mature,[4,7-9] application of MS for determining the dynamics of such interactions has scarcely been undertaken. A notable exception is the work of Krylov and co-workers, who have extracted rate constants from the elution profiles of dissociating protein-ligand complex undergoing separation by CE[10] or size exclusion chromatography[11] followed by MS detection of the ligand.

Time-resolved MS[12,13] involves the rapid mixing of reagents, incubation of the mixture for a variable time, and online or offline MS analysis to provide a powerful tool for characterizing rapid, solution-based processes on a time scale of microseconds to seconds. To date, time-resolved MS has been applied to enzymatic reactions,[14] protein unfolding[15] and protein subunit exchange[16] but not to protein-ligand binding, with the exception of offline monitoring of very slow interactions.[17] Microfluidics can be used to automate multi-step fluidic manipulations with ultra-small volumes, and is thus promising for miniaturizing and integrating the steps required for time-resolved MS. Wilson et al. developed a hybrid capillary/microfluidic reactor for the measurement of millisecond time-scale cytochrome c unfolding[18] and later improved the design for monitoring bottom-up hydrogen/deuterium exchange (HDX).[19] While the adjustment of reaction time needed to be performed manually, and the high flow rates (14 µL/min) were suboptimal for efficient ESI desolvation, the results showed the promise of coupling time-resolved MS with microfluidics for monitoring the dynamics of rapid reactions. The development of a fully integrated, miniaturized and automated microfluidic platform for time-resolved MS-based monitoring of protein-ligand interactions should substantially benefit such kinetic measurements.

a. Environmental Molecular Sciences Laboratory, Pacific Northwest National Laboratory, P.O. Box 999, Richland, Washington, USA, 99352
Email: ryan.kelly@pnnl.gov
b. Biological Sciences Division, Pacific Northwest National Laboratory, P.O. Box 999, Richland, Washington, USA, 99352

Electronic Supplementary Information (ESI) available: [details of any supplementary information available should be included here]. See DOI: 10.1039/x0xx00000x

Here we describe a microfluidic platform (Figure 1) that incorporates protein and ligand introduction channels, a multi-lamellar flow mixer, an automated volume-adjustable incubation chamber, and an integrated electrospray source for time-resolved MS-based monitoring of protein-ligand binding kinetics. The device is fabricated using multilayer soft lithography and consists of three layers: a flow layer, a control layer, and a cover layer (Figure S1). The multi-lamellar flow mixer contains 28 co-flowing channels of alternating composition that merge into a single narrow channel (Figure 1B). The protein introduction channel (Figure 1, blue) is on the flow layer and directly connects to the long co-flowing channels, while the ligand introduction channel (yellow) is part of the cover layer and connects to shorter co-flowing channels via holes punched on the control layer (Figure S1). Figure 1C shows a 3D representation of the connection between the protein and ligand introduction channels and the co-flowing channels of the micro-mixer. The incubation chamber comprises eight flow paths which have a volume range spanning a factor of ~30 (4.5 nL – 120 nL). A photograph of a device interfaced with a mass spectrometer is shown in Figure S2.

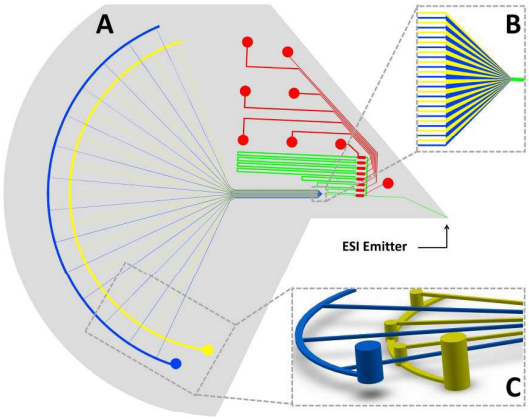

Figure 1. (A) Platform overview with device outline shown in grey. (B) Top view of the multi-lamellar mixer. (C) Side view of the protein and ligand introduction channels. Protein (blue) and ligand (yellow) are introduced via individual inlets and split into 28 coflowing channels of alternating composition. The flow channels merge to induce rapid mixing as shown in the inset, and the mixture passes through a variable flow path (green) with an incubation time that depends on the actuation state of the microvalves (red). Following incubation, the solution is directed to an integrated ESI emitter for MS analysis.

To monitor protein-ligand binding kinetics, the protein and ligand solutions were initially split into two sets of co-flowing channels. Mixing was triggered at the merging triangle and completed in the narrow channel. After rapid mixing, the solution was directed to the incubation channels. The incubation time was determined by the volume of the given flow path, which was selected through the actuation states of the integrated pneumatic microvalves. The mixture was subsequently electrosprayed and detected by an ion mobility spectrometry (IMS)/time-of-flight MS instrument,[20] which was optimized to preserve fragile noncovalent interactions.

Monitoring dynamic, solution-based processes by MS imposes requirements on both fluidic sample handling and detection, and reagent mixing should be as rapid as possible to enable a well-defined starting point. The laminar flow conditions present in microfluidic channels present a challenge for rapid mixing,[21] as the primary mechanism is diffusional mass transport. Reducing the diffusion distance by splitting the flow into several laminae can substantially decrease mixing time.[22,23] Here we integrate a multi-lamellar flow mixer containing 28 co-flowing channels merging into a single narrow channel to reduce the diffusion distance. The average diffusion time *t* of a molecule over a distance *L* is:

$$t = \frac{L^2}{2D}$$

where *D* is the diffusion coefficient of the molecule. For the protein/ligand mixing pair studied here, we consider the diffusion time of carbonic anhydrase (the model protein used for the present study) across the laminar distance as the mixing time since the diffusion coefficient of protein is limiting. The diffusion coefficient of carbonic anhydrase in an aqueous solution can be correlated to its molecular weight, *M* (g/mol), based on an equation proposed by Young *et al.*:[24]

$$D = 8.34 \times 10^{-8} \frac{T}{\eta M^{1/3}}$$

where T is temperature (K), and η is the solvent viscosity (cP). The calculated diffusion coefficient of carbonic anhydrase (29 kDa) at room temperature is 8.0×10^{-11} m^2/s, corresponding to a calculated mixing time of 13 ms for *L*=20/14 µm, which is nearly 200 times faster than a straight channel mixer without co-flowing channels. For visual comparison, the multi-lamellar mixer was compared to a serpentine Y-micromixer using colored dyes. Figure 2A shows the complete mixing of the dyes using the multi-lamellar mixer at a total flow rate of 3 µL/min. In contrast, mixing in a 15-µm-wide serpentine Y-micromixer is incomplete even after 50 ms at the same flow rate (Figures 2B and 2C). The multi-lamellar mixer thus provides rapid and efficient mixing, enabling MS-based monitoring of millisecond protein-ligand binding dynamics.

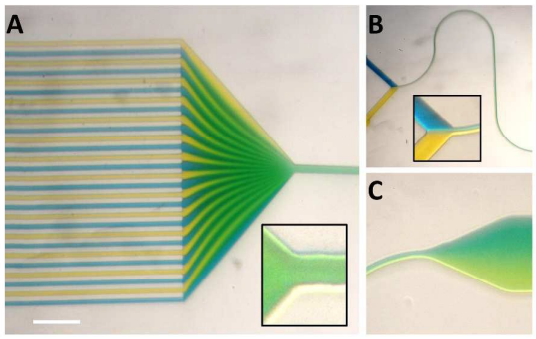

Figure 2. Mixer based on parallel lamination. (A) 28 co-flowing channels of alternating composition are combined in a triangular mixing region that tapers to a 20-um-wide channel. The time to traverse the mixing region is 13 ms. For comparison, the inlet (B) and outlet (C) of a 15-µm-wide serpentine Y-micromixer indicate incomplete mixing after 50 ms. The flow rate was 3 µL/min for all images. Scale bar is 100 µm.

Continuous flow methods are usually used in time-resolved MS for monitoring reaction kinetics.[25] The reaction time can be adjusted in two ways: (1) changing flow rate at a fixed reaction volume,[26] and (2) changing reaction volume at fixed flow rate.[25] For MS detection,

changing flow rate can substantially alter the ionization efficiency of the ESI source, negatively impacting quantitative measurements, and can also destabilize the electrospray. Thus, changing reaction volume at a fixed flow rate is preferred. In our design, the incubation chamber incorporates eight flow paths having different

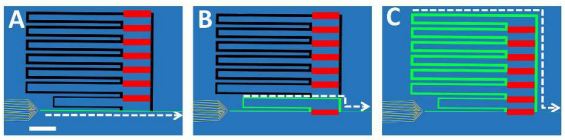

Figure 3. Schematic showing flow-path-based control of incubation time by actuation of the microvalves. (A) The protein/ligand mixture flows through the first flow path with the corresponding microvalve (not shown) open and the others (red) closed. (B) The protein/ligand mixture flows through the second flow path by opening the second microvalve and closing all others. (C) The protein/ligand mixture flow through the longest flow path by opening the corresponding microvalve. Scale bar is 3 mm.

volumes (Figure 3). The reaction time corresponds to the volume of the selected flow path, and the selection of the path is controlled by the actuation state of the integrated pneumatic valves. As such, a wide range of reaction times can be accommodated to follow a process from close to t=0 until equilibrium is reached. Figure 3A shows that the protein/ligand mixture flows through the first flow path by opening the first microvalve and closing the others, with a reaction volume of 4.5 nL and a time of 90 ms at 3 µL/min. Figures 3B and 3C show the protein/ligand mixture passing through the second and eighth flow paths, respectively. By stepping from the first flow path to the eighth flow path, the reaction time increases from 90 ms to 2.4 s at a total flow rate of 3 µL/min.

Human carbonic anhydrase I (hCA-I) is an enzyme that catalyzes the hydration of carbon dioxide to carbonic acid. It has a series of inhibitors that suppress its activity.[27] Furosemide, a drug used to treat fluid build-up due to heart failure, liver scarring, or kidney disease, can quickly inhibit hCA-I via non-covalent interactions in which hydrogen bonding and Van Der Waals interactions play major roles.[28] In this study, carbonic anhydrase-furosemide binding was used to evaluate the microfluidic platform for monitoring millisecond time-scale kinetics. Stable electrospray was achieved by applying an ESI voltage of 4.6 kV at a flow rate of 3 µL/min. The large applied voltage served to minimize the volume of the electrospray Taylor cone, which was found to be ~50 pL in previous work[29] and was thus neglected here when calculating the incubation volume. The integrated emitter is similar to those reported previously,[29-33] which have been found to provide highly stable and long-term performance. While long-term operation of the devices used in the current study was not evaluated, it is expected that neither the emitter nor the valves will be a common source of failure.

Figure 4 shows mass spectra of a mixture of 5 µM hCA-I and 25 µM furosemide at the 10^+ charge state after an incubation time of 90 ms (Figure 4A) and 2.4 s (Figure 4B). The later time point shows a decrease in peak intensity of the native protein and an increase in peak intensity of the protein-ligand complex, indicating more protein/ligand binding with longer reaction times. Note that the secondary peaks are a mixture of nonspecific Zn adducts and Zn-bound hCA-I, and furosemide appears to bind to hCA-I and apo-hCA-I (lacking its cofactor Zn^{2+}) with similar affinity, as has been observed with related systems.[34] Figure 5 shows the binding profiles of carbonic anhydrase at an initial concentration of 5 µM and furosemide at initial concentrations of 25 µM and 50 µM, respectively, also monitored at the 10^+ charge state. The incubation time was adjusted by stepping through the eight flow paths. Protein-ligand binding reached equilibrium at ~1 s with an initial furosemide concentration of 50 µM and at ~1.5 s with 25 µM. As expected, higher initial furosemide concentrations led to faster equilibration and higher concentrations of the protein-ligand complex. The narrow error bars, obtained from 3 separate runs, illustrate the excellent reproducibility of the platform. A simple binding interaction of two biomolecules can be described using the following model:

$$A + B \underset{k_{off}}{\overset{k_{on}}{\rightleftharpoons}} AB$$

When the reaction is at equilibrium, the equilibrium dissociation constant can be expressed as:

$$K_D = \frac{k_{off}}{k_{on}} = \frac{[A][B]}{[AB]}$$

By measuring the ratio of unbound protein to complex based on acquired mass spectra, the relevant concentrations can be obtained at each time point. This assumes that ionization efficiency is not changed upon binding of the ligand,[35] which is reasonable for a large protein and a small ligand as is the present case, and it is possible to verify this assumption or correct for discrepancies as needed with the incorporation of a nonbinding internal standard.[36] With the current system, the K_D of carbonic anhydrase-furosemide binding interactions is calculated as 6.35 µM (standard error of the mean, SEM, of 1.5 µM), which is similar to but somewhat higher than the 2.38 µM obtained by SPR[7]. The calculated on and off rates, obtained by nonlinear curve fitting using Graphpad Prism software

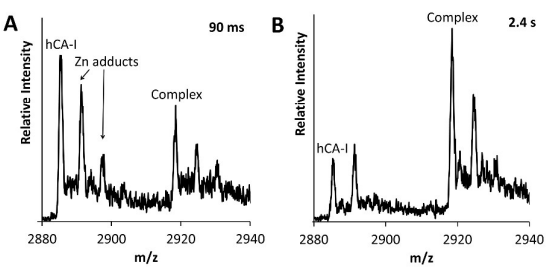

Figure 4. The effect of incubation time on hCA-I-furosemide binding. (A) Mass spectrum of protein/ligand mixture traversing the shortest flow path with an incubation time of ~90 ms with a complex:hCA-I ratio of 0.58 after baseline subtraction. (B) Mass spectrum of the same mixture passing through the longest flow path with an incubation time of ~2.4 s, resulting in an increase in the ratio of complex:hCA-I to 3.0.

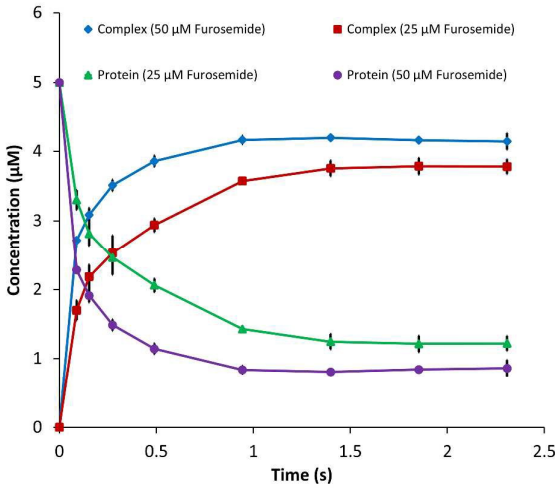

Figure 5. hCA-I-furosemide binding profile monitored by time-resolved MS at the 10+ charge state for an initial concentration of hCA-I of 5 µM. The incubation time was adjusted by stepping through the eight flow paths. Error bars represent the standard error of the mean of three replicate measurements.

(see Supplemental Information), were found to be k_{on} = 1.7×10^5 M^{-1}s^{-1} and k_{off} = 1.07 s^{-1} (SEM = 9.9×10^3 M^{-1}s^{-1} and 0.22 s^{-1}, respectively). These values are also in reasonable agreement with the only published values for this protein ligand system,[7] which were obtained by SPR (k_{on} = 2.12×10^4 M^{-1}s^{-1} and k_{off} = 0.0505 s^{-1}). Potential sources of error with the current system include the different ammonium acetate concentration used in the buffer solutions,[8] the addition of methanol in the buffer solution used to stabilize electrospray, limited gas-phase dissociation of the complex, and artifacts associated with the SPR measurements used for benchmarking.[37] Still, such discrepancies are quite acceptable for these measurements and are considered to be in close agreement.[7]

Conclusions

We have designed a novel microfluidic platform for MS-based monitoring of protein-ligand binding dynamics. The microchip incorporates protein/ligand introduction channels, a multi-lamellar flow mixer for rapid mixing, a novel variable-volume incubation chamber based on pneumatic microvalves, and an on-chip electrospray ionization emitter. The sub-micrometer diffusion distances established by the mixer produce mixing times of around 13 ms. The incubation chamber contains eight flow paths which have different volumes, leading to a range of incubation times from 90 ms to 2.4 s at 3 µL/min total flow rate. The binding kinetic profile of carbonic anhydrase and furosemide was monitored by MS to validate device performance. The result shows a reproducible trend towards equilibrium at longer incubation times. The binding of carbonic anhydrase with an initial concentration of 5 µM reached equilibrium at ~1s with an initial furosemide concentration of 50 µM and at ~1.5 s with 25 µM furosemide.

Further development of the on-chip emitter such as hydrophobic surface treatment should enable stable electrospray without any organic co-solvent since such a solvent can potentially affect the accuracy of the binding measurements. The mixing time can be reduced by increasing the number of the co-flowing channels, and the range of incubation times can be increased by adding more flow paths or varying their volumes. The volume of the region where the co-flowing channels meet can be reduced to minimize pre-mixing before the protein and ligand merge into the narrow single channel. Further reductions in the flow rate (with a concomitant enhancement in ESI-MS sensitivity), which can still achieve rapid mixing and short incubation times, will lead to a broadening of the dynamic range of measurement such that systems having low-nM affinities should become accessible. A final issue is common to all MS-based efforts to study noncovalent interactions, which is the need to ensure that the observed ratios of bound and unbound protein peak intensity accurately reflect the ratios of their concentrations.[7,38] With additional developments such as these, this microfluidic platform should find broad application for monitoring a variety of rapid, label-free and time-resolved processes by MS.

Acknowlegements

The research described in this paper was conducted under the Laboratory Directed Research and Development Program at Pacific Northwest National Laboratory (PNNL), a multiprogram national laboratory operated by Battelle for the U.S. Department of Energy. E.S.B. acknowledges support from the National Institute of Environmental Health Sciences of the NIH (R01ES022190). The research was performed using EMSL, a national scientific user facility sponsored by the Department of Energy's Office of Biological and Environmental Research and located at PNNL.

References

1. S. Niu, J. N. Rabuck and B. T. Ruotolo, *Curr. Opin. Chem. Biol.*, 2013, **17**, 809-817.
2. V. Katritch, V. Cherezov and R. C. Stevens, *Annu. Rev. Pharmacol.*, 2013, **53**, 531-556.
3. K. Vuignier, J. Schappler, J. L. Veuthey, P. A. Carrupt and S. Martel, *Anal. Bioanal. Chem.*, 2010, **398**, 53-66.
4. J. M. Daniel, S. D. Friess, S. Rajagopalan, S. Wendt and R. Zenobi, *Int. J. Mass Spectrom.*, 2002, **216**, 1-27.
5. K. J. Pacholarz, R. A. Garlish, R. J. Taylor and P. E. Barran, *Chem. Soc. Rev.*, 2012, **41**, 4335-4355.
6. M. A. Sowole, S. Vuong and L. Konermann, *Anal. Chem.*, 2015, **87**, 9538-9545.
7. M. C. Jecklin, S. Schauer, C. E. Dumelin and R. Zenobi, *J. Mol. Recognit.*, 2009, **22**, 319-329.
8. A. F. Gavriilidou, B. Gulbakan and R. Zenobi, *Anal. Chem.*, 2015, **87**, 10378-10384.
9. D. Cubrilovic and R. Zenobi, *Anal. Chem.*, 2013, **85**, 2724-2730.
10. M. Kanoatov, L. T. Cherney and S. N. Krylov, *Anal. Chem.*, 2014, **86**, 1298-1305.
11. J. Y. Bao, S. M. Krylova, L. T. Cherney, J. C. Y. LeBlanc, P. Pribil, P. E. Johnson, D. J. Wilson and S. N. Krylov, *Anal. Chem.*, 2014, **86**, 10016-10020.
12. C. Lento, G. F. Audette and D. J. Wilson, *Can. J. Chem.*, 2015, **93**, 7-12.
13. Y. C. Chen and P. L. Urban, *Trac-Trend Anal. Chem.*, 2013, **44**, 106-120.
14. M. D. Robbins, O. K. Yoon, G. K. Barbula and R. N. Zare, *Anal. Chem.*, 2010, **82**, 8650-8657.
15. P. Liuni, B. Deng and D. J. Wilson, *Analyst*, 2015, **14**, 6973-6979.
16. A. J. Painter, N. Jaya, E. Basha, E. Vierling, C. V. Robinson and J. L. P. Benesch, *Chem. Biol.*, 2008, **15**, 246-253.
17. L. Deng, E. N. Kitova and J. S. Klassen, *J. Am. Soc. Mass Spectr.*, 2013, **24**, 49-56.
18. T. Rob and D. J. Wilson, *J. Am. Soc. Mass Spectr.*, 2009, **20**, 124-130.
19. T. Rob, P. K. Gill, D. Golemi-Kotra and D. J. Wilson, *Lab Chip*, 2013, **13**, 2528-2532.
20. E. S. Baker, B. H. Clowers, F. Li, K. Tang, A. V. Tolmachev, D. C. Prior, M. E. Belov and R. D. Smith, *J. Am. Soc. Mass Spectrom.*, 2007, **18**, 1176-1187.
21. K. Ward and Z. H. Fan, *J. Micromech. Microeng.*, 2015, **25**.
22. C. Erbacher, F. G. Bessoth, M. Busch, E. Verpoorte and A. Manz, *Mikrochim. Acta.*, 1999, **131**, 19-24.
23. F. G. Bessoth, A. J. deMello and A. Manz, *Anal. Commun.*, 1999, **36**, 213-215.
24. M. E. Young, P. A. Carroad and R. L. Bell, *Biotechnol. Bioeng.*, 1980, **22**, 947-955.
25. N. Zinck, A. K. Stark, D. J. Wilson and M. Sharon, *Chemistryopen*, 2014, **3**, 109-114.
26. P. V. Attwood and M. A. Geeves, *Anal. Biochem.*, 2004, **334**, 382-389.
27. V. M. Krishnamurthy, G. K. Kaufman, A. R. Urbach, I. Gitlin, K. L. Gudiksen, D. B. Weibel and G. M. Whitesides, *Chem. Rev.*, 2008, **108**, 946-1051.

28. S. Ranjbar, S. Ghobadi, R. Khodarahmi and H. Nemati, *Int. J. Biol. Macromol.*, 2012, **50**, 910-917.
29. R. T. Kelly, K. Tang, D. Irimia, M. Toner and R. D. Smith, *Anal. Chem.*, 2008, **80**, 3824-3831.
30. R. T. Kelly, J. S. Page, I. Marginean, K. Q. Tang and R. D. Smith, *Angew. Chem. Int. Edit.*, 2009, **48**, 6832-6835.
31. X. F. Sun, R. T. Kelly, K. Q. Tang and R. D. Smith, *Analyst*, 2010, **135**, 2296-2302.
32. X. F. Sun, R. T. Kelly, K. Q. Tang and R. D. Smith, *Anal. Chem.*, 2011, **83**, 5797-5803.
33. X. F. Sun, K. Q. Tang, R. D. Smith and R. T. Kelly, *Microfluid. Nanofluid.*, 2013, **15**, 117-126.
34. J. M. Gao, Q. Y. Q. Wu, J. Carbeck, Q. P. Lei, R. D. Smith and G. M. Whitesides, *Biophys. J.*, 1999, **76**, 3253-3260.
35. B. Gulbakan, K. Barylyuk and R. Zenobi, *Curr. Opin. Biotech.*, 2015, **31**, 65-72.
36. V. Gabelica, F. Rosu and E. De Pauw, *Anal. Chem.*, 2009, **81**, 6708-6715.
37. R. L. Rich and D. G. Myszka, *Curr. Opin. Biotech.*, 2000, **11**, 54-61.
38. E. N. Kitova, A. El-Hawiet, P. D. Schnier and J. S. Klassen, *J. Am. Soc. Mass. Spectr.*, 2012, **23**, 431-441.